Australian Journal of Crop Science AJCS

Aust J Crop Sci. 18(10):658-665 (2024) | ISSN:1835-2707
https://doi.org/10.21475/ajcs.24.18.10.p60

Estimation of common bean (cultivar BRS Estilo) crop evapotranspiration by remote sensing using different albedo sources

Fillipe de Paula Almeida, José Alves Júnior*, Fábio Miguel Knapp, João Maurício Fernandes Souza, Antonio Heriberto de Castro Teixeira, Adão Wagner Pêgo Evangelista, Derblai Casaroli, Rafael Battisti

School of Agronomy, Department of Soil and Water, Federal University of Goiás (UFG), Zip code 74.690.900, Goiania, Goiás, Brazil

***Corresponding author: José Alves Júnior** ✉

Submitted: *30/11/2023*

Revised: *18/06/2024*

Accepted: *21/06/2024*

Abstract: Evapotranspiration (ET) estimation by remote sensing is an innovative and promising option, due to its low cost and operation. It is an important tool for estimating ET and can be used to support decision-making. The origin and quality of images are fundamental for quality of information, as low spatial and temporal resolution of satellites directly impacts these customers. In this context, the objective of this study was to estimate the evapotranspiration of common bean crop using the SAFER algorithm in three different sources of albedo. The study was carried out in a bean cultivation area irrigated by central pivot, located in Itaberaí-GO Brazil in 2021. Images from a MicaSense Altum multispectral and thermal camera coupled to a drone and albedo images from Landsat 8 and Sentinel 2A satellites were used for ET_a estimation. The data were compared with ET met by FAO method, Embrapa and climatological water balance by statistical indices. The correlation with standard methods was satisfactory, especially with FAO, and in general, the MSE (mean square error) and MAE (mean absolute error) adopted values smaller than 0.4mm day^{-1}. The confidence index ranges from 0.91 to 0.97. The comparison of the ET values calculated from the multispectral and thermal camera and the three ways of calculating the surface albedo was considered satisfactory. Thus, the adaptation adopted in the SAFER algorithm for obtaining the albedo was efficient. The use of multispectral and thermal camera images with SAFER is an efficient tool in estimating the evapotranspiration of bean crop, and is capable of replacing the use of orbital images, which are limited by meteorological conditions and imaging frequency.

Keywords: *Drone;* energy balance; geoprocessing; orbital images

Introduction

Beans is very important to human nutrition, as a cheap source of carbohydrates and proteins (Chaves and Bassinelo, 2014). Common beans (*Phaseolus vulgaris* L.) are one of the main legume crops in the world, with Brazil being the largest producer (FAO, 2021). Brazil consumes a large part of the beans produced on the domestic market and therefore does not have a large global export volume (FAO, 2021).

Goiás State has the third largest national production (IBGE, 2021). Despite the large production, average productivity is still low. Among the various factors that cause a drop in productivity (fertilization, phytosanitary control, genetics), water deficit is one of the most important. Within this scenario, it is essential to know the evapotranspiration (ET) of the bean crop, to estimate productivity and loss of productivity. Because, it is widely cultivated during the rainy season and the summer season directly influences these losses.

Brazil is among the ten countries with the largest irrigated area in the world, in the country the bean crop is among the five most irrigated (ANA, 2021). In relation to the entire irrigated area in the country, Goiás is among the four states that hold 80% of this volume (ANA, 2021). To protect against water deficit and phytosanitary problems, beans are also produced in the winter harvest, using irrigation. In which, refined information on crop evapotranspiration is fundamental for water resources management, project sizing and irrigation management.

According to Coelho Filho et al. (2011) ET can be defined as the sum of water losses from a surface covered by vegetation to the atmosphere. This sum is made up of evaporation from the soil surface and plant transpiration. Therefore, accurately quantifying ET is essential in irrigation management, generating savings in water resources, avoiding losses due to diseases and pests, in addition to supporting decision-making.

ET can be obtained using the direct lysimetry method or indirect methods. Among indirect methods, remote sensing has been studied and recommended for several crops, such as beans (Sales et al., 2016); tomato (Sales et al., 2017 and Sena, 2020); sugarcane (Sousa et al., 2020, Mussi et al., 2020 and Alves Jr. et al., 2023), lawn (Aldrighi et al., 2020) and corn (Teixeira, 2021). It consists of carrying out an energy balance, with data obtained from orbital or drone images. This energy balance is calculated through energy flows that occur between soil, vegetation and the atmosphere, requiring an algorithm to obtain this data (Bezerra et al., 2008). Among these algorithms, SAFER (Simple Algorithm For Evapotranspiration Retrieving) developed by Teixeira et al. (2012) stands out for its practicality.

SAFER is an algorithm developed to be easy to apply, it is simplified and does not require the use of the thermal band,

Figure 1. Location map of the study area. Typical bean production area in the region, Itaberaí, Goiás, Brazil.

and can therefore be used on a wider range of satellites. It requires data from a meteorological station close to the area of interest, to obtain reference evapotranspiration (ETo), global radiation (Rg) and average air temperature (Ta). Together with the parameters obtained by remote sensing, the current evapotranspiration (ETa) and the current crop coefficient are obtained.

However, many authors warn about the low frequency of images from the Landsat 8 and Sentinel 2A satellites (16 and 10 days, respectively). Furthermore, all satellite measurements require cloud-free sky conditions (Cao et al., 2018). This problem can be solved with the use of multispectral and thermal cameras attached to drones. However, for this is necessary to create alternatives to obtain the surface albedo, so as not to depend on this variable coming from satellite images.

Surface albedo is a key parameter in energy balance. It varies according to changes in vegetation morphology throughout the seasons and is affected by atmospheric conditions (Liang, 2021). Albedo, NDVI and surface temperature are the three variables responsible for calculating evapotranspiration using the SAFER algorithm. This demonstrates the need to obtain reliable albedo data.

Therefore, the objective of this study was to evaluate the impact of different sources of albedo in bean crops on the estimation of ET using remote sensing, through images from a multispectral and thermal camera attached to a drone.

Results and discussion

Weather, soil and harvest data

During the cycle the average temperature was 23.55 °C, an average favorable to the development of the culture. During the seed germination period, temperatures around 28°C are considered optimal, between emergence and physiological maturation it should be between 12°C and 30°C (Didonet and Silva, 2004). Accumulated precipitation was 73.45 mm, irrigation was 226.25 mm, totaling 299.7 mm during the entire cycle (Table 1).

The harvest began on October 22, 2021, totaling 106 days of cycle. Productivity was 3.13 t ha-¹, 8% above the average for the 3rd harvest for Goiás (CONAB, 2022). Tables 2 and 3 illustrate average values for soil density and penetration resistance per layer. The study area did not present compaction problems.

Levels of phosphorus (P) and magnesium (Mg) were found in the leaf samples. The average level of P in the samples was 1.63 g kg^{-1} and of Mg was 2.8 g kg^{-1}. According to Malavolta et al. (1997) sufficient levels are between 2-3 g kg^{-1} and 4-7 g kg^{-1}, respectively. Figure 2 represents the temporal variation in soil moisture and precipitation and irrigation during the bean crop cycle. It is possible to observe that the humidity values did not fall below the critical point at any time and in any layer during the entire cycle.

Albedo

For atmospheric correction of the data, a linear correlation was performed between the albedo data obtained by the albedometer and the albedo at the top of the atmosphere by Sentinel 2A. According to Equation 15:

$$\alpha_0 = 0.7184 * \alpha\ top + 0.008 \quad (15)$$

Thus, the coefficients "a" and "b" were obtained for estimating the surface albedo, 0.7184 and 0.008, respectively. For Landsat 8 the values are already calibrated according to Teixeira (2010). Equation 16 represents the calibration of the drone's albedo as a function of the albedometer:

$$\alpha_0 = 1.0283 * \alpha_{albedômetro} + 0.0117 \quad (16)$$

Crop evapotranspiration

At the beginning of the cycle, there was a large amount of straw, which made it difficult to obtain evapotranspiration by drone. The resolution of the thermal band (160 x 120) is lower compared to the other bands (2064 x 1544). This caused a greater superimposition of the temperature between the lines over the lines, tending to underestimate the kc. To alleviate this problem, a selection of pixels was made, so that these hottest areas were left out of the algorithm's calculation.

Figure 3 illustrates the kc curve during the bean crop cycle. It is possible to observe that the highest values among the drone data were by the $Drone_{Alb}$ and $Drone_{Sat}$ methods, as the data obtained by the albedometer were close to those obtained by satellite, resulting in higher kc values.

Many authors emphasize the underestimation of ET by satellite images at the beginning of the cycle for several crops. According to Oliveira et al. (2021) this process occurs

Table 1. Accumulated thermal, precipitation (rain fall), ETo and bean irrigation depth for the area evaluated in 2021.

Accumulated Thermal*	Precipitation Rain Fall	ET_o	Irrigation Depth
°C	----------mm----------		
1,397.88	73.45	422.29	226.25

*According with Ometto (1981).

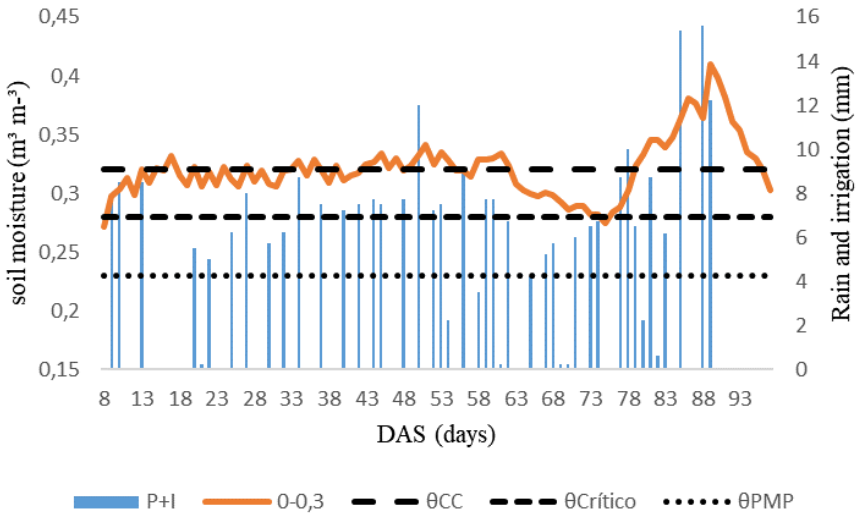

Figure 2. Temporal variation of soil moisture in the 0.0-0.3 m soil layers and precipitation (rainfall) with irrigation depth.

due to the presence of straw, which influences low NDVI values (due to the color of the material, NDVI responds better to different shades of green), in addition to the influence on albedo, which due to the spatial resolution of the image does not differentiate the plant straw. This same effect was reported by Sales et al. (2017) for tomato cultivation and Sales et al. (2016) for bean cultivation. However, this effect was not observed for the area because there was no data at the beginning of the cycle.

Table 4 and Supplementary Figure 1 detail the evapotranspiration values and the statistical indices of the estimation of the $ET_{DroneAlb}$, $ET_{DroneSat}$ and ET_{Drone} methods in comparison with the FAO 56, Embrapa and BHC method. From the results, the data estimated by drone with different albedo sources can be used to estimate the evapotranspiration of bean crops, as they obtained low error and high correlation. Overall, on average the EQM was 0.215 mm day^{-1}, EMA was 0.332 mm day^{-1} and REMA was 0.096 mm day^{-1}.

The fact that the crop is under a direct planting system influenced the low error observed between the methods, as the straw retains moisture and maintains a lower temperature in the soil. Among the drone methods, the mean square error (MSE) had an overall average of 0.137 mm day^{-1}, the mean absolute error (EMA) had an average of less than 0.3 mm day^{-1}. The root mean absolute error (REMA) had an overall average of 0.061. It is also possible to observe that the curves generated throughout the cycle for all methods follow the same trend.

The values obtained by the study using the drone are close to those recommended by Allen et al. (1998) for bean cultivation. This proves the efficiency of using SAFER with drone images. The confidence index ranged from 0.93 to 0.97. The data obtained in this study are also in accordance with Embrapa (Stone et al., 2006), which recommended kc for bean cultivation in direct planting conditions and edaphoclimatic conditions in the Cerrado.

In comparison with the climatological water balance, the three methods with drone images obtained an "excellent" rating, the confidence index ranged from 0.91 to 0.95. According to Queiroz et al. (2022), this can be explained by the low amount of data, due to the occurrence of clouds and low temporal resolution of the sensor.

The comparison of ET between the three methods of obtaining albedo showed a high correlation, proving that the adaptation promoted in the algorithm is efficient. Therefore, there is no dependence on weather conditions on the day of the flight, clouds do not influence the albedometer reading and drone images. In general, $ET_{DroneAlb}$ presented the best result among all methods to estimate ET. This was due to higher albedo values during most of the cycle.

It is possible to observe in Figure 4A the variation in surface temperature estimated by the drone. The spatial resolution of the thermal camera when compared to the Landsat 8 satellite, for example, is around 4,100 times greater, it is able to separate the temperature between the lines and the lines, resulting in better values. Nádudvari et al. (2020), researching fire outbreaks using images from Landsat 8 and a thermal camera attached to a drone, concluded that due to better spatial resolution, drone images capture better temperature values. However, there is no historical database of these images, so the two image sources are complementary.

In Figure 4B it is possible to observe the growth of NDVI values until the beginning of the reproductive period, during this period the values remained stable until the decrease began from the beginning of senescence.

Figure 5 represents the variation in albedo throughout the bean cycle. The highest values are between the albedometer and Sentinel 2A. In general, the albedo values estimated from the drone images presented the lowest values compared to other albedo sources, which represented a greater error when comparing the drone methods in relation to the reference models. Dittmann et al. (2019) states that satellite measurements have spatial and temporal limitations, hence the need to calibrate the data with the albedometer.

It is possible to observe higher albedo values at the beginning and end of the cycle. Leite et al. (2020), researching the variation in surface albedo in different soil covers, emphasizes that areas such as exposed soil and dry vegetation have high reflective power, that is, high albedo. Giongo and Vettorazzi (2014) mapped the albedo of a river

Table 2. Average values of soil density, granulometry and texture per layer.

Layer (m)	Soil density (g cm^{-3})	Granulometry (%)			Texture[1]
		Sandy	Silt	Clay	
0.0-0.1	1.48	61.25	10.1	28.65	sandy clay loam
0.1-0.2	1.49	55.75	11	33.25	sandy clay loam
0.2-0.3	1.44	53.5	10.3	36.2	Sandy clay

[1]According with Lemos and Santos (1996).

Table 3. Average values of soil resistance to penetration and volumetric moisture per layer.

Layer (m)	RP (Mpa)	Uv (cm^{-3} cm^{-3})
0.0-0.1	0.62	0.23
0.1-0.2	1.51	0.25
0.2-0.3	2.13	0.21

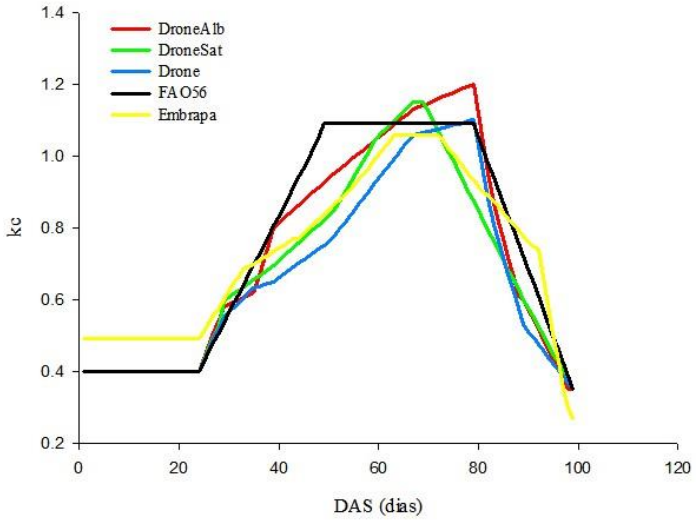

Figure 3. Comparison of kc estimated by the FAO, Embrapa, DroneAlb, DroneSat and Drone method, throughout the bean cycle, Itaberaí-GO, BRAZIL, 2021.

basin and concluded that the highest values of the index are in areas with little or no vegetation cover, in addition to agricultural areas, which had exposed soil.

Supplementary Table 1. shows the statistical indices for estimating $ET_{DroneAlb}$, $ET_{DroneSat}$, ET_{Drone}, by phase in comparison between the methods themselves and with the FAO 56, Embrapa and BHC methods. For phase I, the comparison was not carried out, due to the sowing being carried out in a direct planting system, several corn seeds emerged, thus the plants stood out from the bean ones. Subsequently, herbicide was applied, which turned the leaves of the corn plants yellow, which could interfere with the results.

In general, the methods estimated by drone can be used to obtain the evapotranspiration of the bean crop, the correlation varied from good to excellent, as they obtained low error and good agreement.

For phase II, $ET_{DroneAlb}$ showed better performance compared to FAO, presenting an EQM value of 0.089 mm day^{-1}, EMA 0.242 mm day^{-1} and REMA 0.065 mm day^{-1}. It obtained statistical indices above 0.9, obtaining an "excellent" rating. $ET_{DroneSat}$ obtained a "very good" rating, obtaining r = 0.89, d = 0.85 and c = 0.76. ET_{Drone} presented NDE and EMA above 0.5 mm day^{-1}, being classified as "good".

In comparison with Embrapa in phase II, $ET_{DroneSat}$ and ET_{Drone} performed better, presenting an average EQM of 0.071 mm day^{-1}, EMA 0.242 mm day^{-1} and REMA 0.078 mm day^{-1}, with an "excellent" rating. The $ET_{DroneAlb}$ data received a "very good" rating, with r = 0.89, d = 0.93 and c = 0.83.

Still in phase II, compared to BHC, ETDroneAlb achieved better performance, classified as "excellent", with EQM of 0.104 mm day^{-1}, EMA 0.274 mm day^{-1} and REMA 0.086 mm day^{-1}. $ET_{DroneSat}$ and ET_{Drone} presented a "good" and "very good" rating, with a confidence index below 0.8. The comparison between the three drone methods obtained a correlation from "very good" to "excellent", low error and good statistical performance, justifying the use of both albedo sources for this phase of development.

In phase III, which coincides with the greatest water demand of the crop, $ET_{DroneAlb}$ presented better performance, classified as "very good" in comparison with FAO, presenting EQM of 0.144 mm day^{-1}, EMA 0.335 mm day^{-1} and REMA 0.064 mm day^{-1}. The indices were r = 0.88, d = 0.92 and c = 0.81. $ET_{DroneSat}$ also showed a good correlation, being classified as "good", with a confidence index close to 0.7. The ET_{Drone} method was not recommended for this phase, it was classified as "average".

In comparison with Embrapa, all methods are recommended, as they were classified from "very good" to "excellent". The methods that obtained the lowest error were $ET_{DroneSat}$ and ET_{Drone}.

Still in phase III, in comparison with BHC, $ET_{DroneAlb}$ showed better performance, with EQM of 0.237 mm day^{-1}, EMA 0.423 mm day^{-1} and REMA 0.089, classified as "very good". ET_{Drone} is also recommended, it received a "good" rating. $ET_{DroneSat}$ was considered to be underperforming.

For phase IV, both drone methods were recommended to FAO, Embrapa and BHC, they were classified from "very good" to "excellent".

The biggest limitation of estimating evapotranspiration using orbital images is the presence of clouds, when present in the observed area, making the estimate for that date

Table 4. Mean square error (MSE, mm day-1), mean absolute error (EMA, mm day-1), root mean absolute error (REMA, mm day-1), correlation coefficient (r), index of agreement (d) and confidence index (c) for the evapotranspiration values obtained by the DroneAlb, DroneSat, Drone methods, comparing them to the ETFAO, ETEmbrapa and ETBHC methods.

Method	EQM	EMA	REMA	r	d	c	Classification
			FAO				
Drone Alb	0.168	0.286	0.066	0.98	0.99	0.97	Great
Drone Sat	0.227	0.330	0.080	0.97	0.97	0.95	Great
Drone	0.339	0.377	0.091	0.96	0.96	0.93	Great
Embrapa							
Drone Alb	0.215	0.389	0.132	0.97	0.98	0.95	Great
Drone Sat	0.126	0.277	0.105	0.98	0.98	0.96	Great
Drone	0.204	0.369	0.131	0.97	0.97	0.94	Great
			BHC				
Drone Alb	0.169	0.292	0.082	0.97	0.98	0.95	Great
Drone Sat	0.253	0.355	0.096	0.94	0.96	0.91	Great
Drone	0.242	0.314	0.084	0.95	0.97	0.92	Great
			Drone Alb				
Drone Sat	0.155	0.231	0.054	0.98	0.98	0.96	Great
Drone	0.158	0.292	0.070	0.99	0.98	0.97	Great
Drone Sat							
Drone	0.099	0.228	0.059	0.98	0.99	0.96	Great

unfeasible. The use of drone images using the satellite's albedo presents good results, but is still limited by clouds. The correlation between the kc data for the drone, using albedo data from the satellite and the albedometer, shows a high correlation. Therefore, the proposal to promote the adaptation of the albedo variable of the algorithm becomes viable, as the presence of clouds is irrelevant at the time of data collection.

Materials and Methods

Location and environmental characteristics

The study was an area of 18 hectares irrigated by central pivot. It is located in Itaberaí-GO, Brazil, 49° 43' 05" W and 16° 01' 30" S (Figure 1). The region's climate is characterized according to Koppen's classification as Aw, with two well-defined seasons, dry winter and rainy summer.

Beans cultivar BRS Estilo were sown on July 8, 2021 in a direct planting system, following corn, with a spacing of 0.5 m between rows and 10 plants per linear meter. Sowing fertilization was carried out with granulated MAP (11-52-00) 0.03 t ha^{-1}, fertilizer (13-33-00 + 15% S) 0.015 t ha^{-1} and fertilizer (10-46-00 + 9 % S) 0.06 t ha^{-1}. The soil was classified as Red Oxisol of medium texture (Embrapa, 2018).

Undisturbed soil samples were collected in volumetric rings at eight georeferenced points in layers 0.0-0.1; 0.1-0.2 and 0.2-0.3 m. Soil density and texture were obtained according to Embrapa (2017). Data on soil resistance to penetration was also collected using a FALKER digital impact penetrometer. The limits of field capacity and permanent wilting point were defined according to Medrado and Lima (2014).

Leaf analysis was carried out to determine macro and micronutrients according to the Embrapa (2000). They were collected during the flowering period, removing the first fully expanded leaf from the upper leaflets (Malavolta et al., 1997).

Treatments and conduction of study

The reference evapotranspiration (ETo) was obtained by the Penman Monteith method, using data from the automatic weather station installed within a radius of 10 meters from the center pivot. The calculation of ETo is described in Equation 4.

$$ET_0 = \frac{\left[0.408 * (Rn - G) + \left[y * \left(\frac{900}{T + 273}\right) * u^2 * (es - ea)\right]\right]}{\Delta + y * (1 + 0.34 * u_2)} \quad (1)$$

Where, Rn corresponds to the radiation balance on the surface of the crop (MJ / m² / day); G is the soil heat flux density (MJ/m²/day); T is the daily average temperature of a (°C); u_2 is the wind speed at 2 meters height (m/s); ES is the air saturation vapor pressure (kPa); ea is the current vapor pressure of the air (kPa); es – ea is the air saturation vapor pressure deficit (kpa); Δ is the slope of the air vapor pressure curve in the atmosphere (kPa / °C) and y is the psychrometric constant (kPa / °C).

With the data for preparing the climatological water balance, the methodology of Thornthwaite and Mather (1955) was used. Considering the data on the pedotransfer function, soil density and effective depth of the root system (Z=0.3 m), the value of 40 mm was used for available water capacity (CAD). By accounting for water inputs and outputs from the system, ETr was estimated during the bean crop cycle.

To estimate the variation in humidity in the soil profile, three sensor batteries were installed, each battery containing three EC-5 sensors from Decagon Devices, in layers 0.0-0.1, 0.1-0.2 and 0.2-0.3 m connected to an EM-50 datalogger, with a reading interval every 20 minutes. To obtain precipitation and irrigation, two tilting rain gauges with 0.25 mm resolution were installed, connected to a (NOVUS) infrared datalogger, with readings every 24 hours. The methodology of Sena et al. (2020) was used to calibrate sensor data according to soil texture.

Field visits were carried out every day that the Landsat-8 and Sentinel-2A satellites passed, every 16 and 10 days respectively, according to the temporal resolution of each sensor. The dates were: 26/jul; 05/Aug; 11/Aug; 15/Aug; 25/Aug; 27/Aug; 05/Sep for Landsat-8 and 12/Sep; 14/Sep; 24/Sep; 28/Sep; 04/Oct; 14/Oct for Sentinel-2A.

To obtain the surface albedo, images from the Landsat-8 satellite (OLI/TIRS) were used, obtained free of charge on the United States Geological Survey (USGS) website. Images from the Sentinel-2A satellite were also used, obtained from the Copernicus website (European Space Agency). On the same date as the satellites' passage and close to the passage time, a flight was carried out with a drone model DJI Inspire 2, coupled with a multispectral and thermal camera model Micasense Altum.

The flight height used was 120 meters for better flight autonomy, generating spatial resolution of 0.6 m. The Pix4D capture software was used to create the flight plan and the Pix4D mapper was used to mosaic the images and obtain

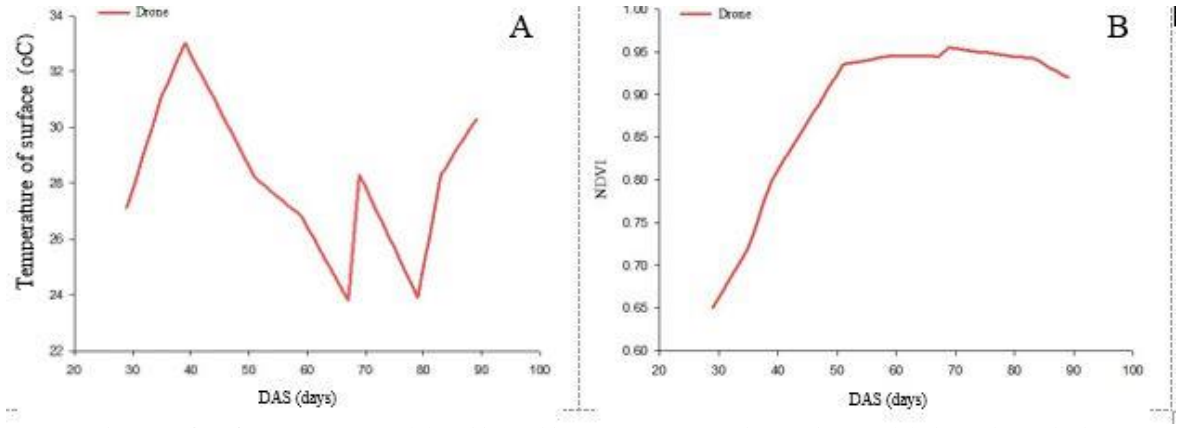

Figure 4. Distribution of surface temperature (A), calibrated by equations 16 and 17 and NDVI (B) throughout the bean crop cycle obtained by images from the Landsat 8 satellite, Sentinel 2A and multispectral and thermal camera.

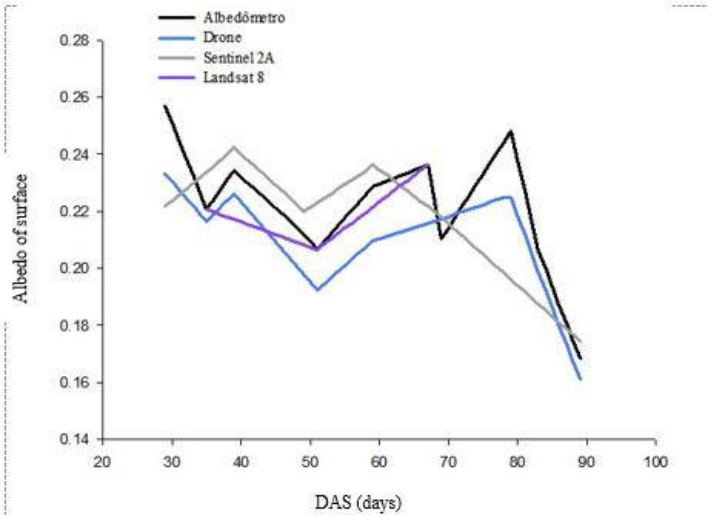

Figure 5. Distribution of surface albedo throughout the bean crop cycle obtained through images from Landsat 8 and Sentinel 2A satellites (corrected by equation 15), multispectral and thermal camera and albedometer.

images in reflectance and NDVI (Normalized Difference Vegetation Index) and surface temperature.

Algorithm used

To obtain evapotranspiration using the SAFER algorithm, it is necessary to follow some steps. These steps follow the methodology proposed by Teixeira (2010).

Conversion of DN values (digital numbers) into radiance

The DN represents a pixel that contains the intensity of electromagnetic energy measured by the satellite sensor. These digital values need to be converted into spectral radiance for each band. Therefore, radiance is the radiant intensity per unit of source area (Mussi et al., 2020).

$$L\lambda = \left(\frac{\text{LMAX}-\text{LMIN}}{255}\right) \text{Q}_{\text{CAL}} + \text{L}_{\text{MIN}} \quad (2)$$

Where:
LMAX: maximum radiance (W m^{-2} sr^{-1} μm^{-2});
LMIN: minimum radiance (W m^{-2} sr^{-1} μm^{-2});
Qcal: pixel intensity (ND), integer from 0 to 255.

Reflectance calculation

For each thermal band contained in the orbital images, the reflectance (Pλ) is calculated from the radiance values that were obtained in the previous step. Reflectance is the process by which radiation passes through an object such as a cloud or a body of water.

$$P\lambda = \frac{\pi * L\lambda}{\text{ESUN}_{\lambda} * \text{cosZ} * \text{E}_0} \quad (3)$$

Where:
Lλ: radiance of each band;
ESUN λ: spectral irradiance at the top of the atmosphere;
cosZ: zenith angle;
Eo: daily angle;

Where: Eo is defined by the Equation:

$$E_0 = 1.000110 + 0.0342221\cos(\text{da}) + 0.001280\,(\text{da}) + 0.000719(2 * \text{da}) + 0.000077\sin(2 * \text{da}) \quad (4)$$

Where:
da: daily angle

Where: da is defined by Equation 8:

$$\text{da} = (d_n - 1)\frac{2\pi}{365} \quad (5)$$

Where:

dn: Julian day of the image

Albedo at the top of the atmosphere

The albedo at the top of the atmosphere can be obtained from the following equation:

$$\alpha_{top} = \Sigma\ (\omega p \times p\lambda) \quad (6)$$

In which:

pλ: reflectance

ωλ: coefficient for each band

Therefore, ωλ is obtained by the equation:

$$\omega\lambda\ = \frac{ESUN_{\lambda}}{\Sigma\ ESUN_{\lambda}} \quad (7)$$

Surface albedo

In SAFER, the surface albedo (α0) was estimated from the albedo at the top of the atmosphere by the following equation:

$$\alpha_0\ =\ a\ *\ \alpha\ top\ +\ b \quad (8)$$

Where: a and b are regression coefficients Teixeira (2010), which present, respectively, values of 0.7 and 0.006, α top, is the albedo at the top of the atmosphere.

Surface temperature

To prepare the surface temperature map (To), it is necessary to use thermal infrared images of the bands, which will be determined later. But the surface temperature is calculated by the equation:

$$To = 1.11\ x\ T_{bright} - 31.89 \quad (9)$$

Where T_{bright} is obtained by the equation:

$$T_{bright} = \frac{1260.56}{\ln\left(\frac{607.76}{\mathrm{L_{termal}} + 1}\right)} \quad (10)$$

Where: L_{termal} = radiance (Lλ) of the bands that will still be chosen.

Normalized Difference Vegetation Index (NDVI)

$$NDVI = \frac{IVP - V}{IVP + V} \quad (11)$$

Where IVP is the reflectance in the near-infrared band and V is the reflectance in the red band.

Equation 12 is used to obtain the current evapotranspiration (ETa) (Teixeira, 2010):

$$\frac{ET}{ETO} = \exp\left[a + b\left(_{\infty *}\ ^{To}_{\mathrm{NDVI}}\right)\right] \quad (12)$$

where, a and b are regression coefficients; where a = 1 (Teixeira et al., 2013) and b = -0.008.

Using the ETa/ETo relationship, we arrive at the value of the crop coefficient. The respective crop coefficients (kc), by SAFER, were calculated using Equation 16:

$$kc = \frac{ETa}{ETo} \quad (13)$$

The way the surface albedo estimation is described in the algorithm, it is not possible to carry out the process with drone images, as the albedo at the top of the atmosphere is taken into account, which the drone does not capture because it is under the top. of the atmosphere. As an alternative, an albedometer model CMA 6 Kipp and Zonen was installed in the field to estimate the data. Furthermore, according to Planck's law (Planck, 1901), the drone's albedo was obtained from the definition of weights per band and subsequently the sum of all bands in reflectance, from Equation 17:

$$\alpha_0 = 0.24 * Blue + 0.23 * Green + 0.2 * Red + 0.14 * NIR + 0.18 * RedEdge \quad (14)$$

Statistical analysis

The albedo obtained by satellites was also used in order to compare the results. A linear regression of the albedometer data was performed with the satellites and drone. Subsequently, the raster calculator tool of the ArcGis 10.3 software was used to calculate evapotranspiration.

The data was correlated with the climatological water balance method (Thornthwaite and Mather (1955), FAO 56 (Allen et al., 1998) and Embrapa (Stone et al., 2006). The FAO data were calibrated to the air humidity and wind speed conditions of the study area, as described in the bulletin. Pearson correlation (r), linear regression (R^2), confidence index (c) and Willmott index "d" were used. This index varies from 0 to 1, the closer it is to 1, the more the estimated values fit the measured values (Willmott et al., 1985).

Conclusions

The different sources of albedo directly influence the evapotranspiration values of the bean crop.

The DroneAlb method in general presents better ET values among the drone methods, as it directly uses the albedometer values, while the other methods are corrected by the albedometer.

When used with multispectral and thermal camera images, SAFER is capable of replacing the use of orbital images, which are limited by meteorological conditions and imaging frequency.

Both drone methods are recommended for estimating ET for bean crops.

References

Allen RG, Pereira LS, Raes D, Smith M (1998) Crop evapotranspiration: Guidelines for computing crop water requirements. Irrig. Drain., Paper: 56, Rome, 297.

Aldrighi M, Jardim CCS, Alves Jr J, Battisti R, Casaroli D, Evangelista AWP (2020) Necessidades hídricas das gramas batatais (*Paspalum notatum Fluggé*) e esmeralda (*Zoysia Japônica Steud*) estimadas por sensoriamento remoto. Braz. J. Dev., Curitiba, 6 (7) 47020-47032.

ANA (2021) Agência nacional de águas e saneamento básico. Atlas Irrigação 2021. Disponível em: < https://biblioteca.ana.gov.br/ Acesso em: 04 de setembro de 2022.

Alves Jr J, Jardim CCS, Casaroli D, Evangelista AWP, Battisti R (2023) Assessment of orbital sensors in estimating sugarcane crop evapotranspiration with the SAFER algorithm. Aust. J. Crop Sci., 17 (11) 761-769.

Bezerra BG, Silva BB, Ferreira NJ (2008) Estimativa da evapotranspiração real diária utilizando-se imagens digitais TM - Landsat 5. Rer. Bras. Meteor., São José dos Campos, 3 (1) 305-317.

Cao C, Lee X, Muhlhausen J, Bonneau L, Xu J (2018) Measuring Landscape Albedo Using Unmanned Aerial Vehicles. Remote Sens., Basel, 10 (1) 1-16.

Chaves MO, Bassinello PZ (2014) O feijão na alimentação humana. Embrapa Arroz Feijão. Disponível em: <ainfo.cnptia.embrapa.br. Acesso em: 20 de maio de 2022.

Coelho Filho MA, Pereira FAC, Angelucci L R, Coelho E F, Oliveira G X S (2011). O processo de evapotranspiração. In: Sousa VF, Marouelli WA, Coelho EF, Pinto JM, Coelho Filho MA. (Ed.). Irrigação e fertirrigação em fruteiras e

hortaliças. Brasília: Embrapa Informação Tecnológica, 91-113.

CONAB (2022) Companhia Brasileira de Abastecimento. *Acompanhamento da safra brasileira de grãos 2021/2022*: 4º levantamento, janeiro de 2022, 2022. Disponível em: https://www.conab.gov.br. Acesso em: 27 de janeiro de 2022.

Didonet AD, Silva SC (2004) Elementos climáticos e produtividade do feijoeiro. Inf. Agrop., Santo Antônio de Goiás, 25 (223) 13-19.

Dittmann S, Burnham L, Oh SY, Benlarabi A, Choi, JH, Ebert M, Figgis B, Gottschalg R, Kim KS, Reindl T, Rüther R (2019) Comparative analysis of albedo measurements (plane-of-array, horizontal, satellite) at multiple sites worldwide. Abstract 36th EU PVSEC, Marseille, SAND2019-1766C.

EMBRAPA (2000) - Empresa Brasileira de Pesquisa Agropecuária. Métodos de Análise de Tecidos Vegetais Utilizados na Embrapa Solos. Rio de Janeiro: Centro Nacional de Pesquisa de Solos, 21 ed., 41.

EMBRAPA (2017) Empresa Brasileira de Pesquisa Agropecuária. Manual de métodos de análise de solo. Rio de Janeiro: Centro Nacional de Pesquisa de Solos, 3 ed. ver. e ampl. 212.

EMBRAPA (2018) Empresa Brasileira de Pesquisa Agropecuária. Centro Nacional de Pesquisa de Solos. Sistema brasileiro de classificação de solos. 5 ed. Brasília, Produção de Informação, 2018. 356.

FAO (2021) Food and Agriculture Organization of the United Nations. Disponível em: http://www.fao.org. Acesso em: 30 ago. 2022.

Giongo PR, Vettorazzi CA (2014) Albedo da superfície por meio de imagens TM-Landsat 5 e modelo numérico do terreno. Rev. Bras. Eng. Agr. Amb., Campina Grande, 18 (8) 833-838.

IBGE (2021) Instituto Brasileiro de Geografia e Estatística. Produção Agrícola Nacional. Sistema IBGE de Recuperação Automática- SIDRA, 2021 Disponível em https://sidra.ibge.gov.br/tabela/5457. Acesso em: 19 de fevereiro de 2022.

Leite ME, Silva LAP, Veloso GA, Magalhaes Filho R (2020) Comportamento e influência do albedo e temperatura de superfície no balanço de radiação em áreas de Cerrado. Caminhos de Geografia, Uberlândia, 21 (733) 131-147.

Lemos RC, Santos RD (1996) Manual de descrição e coleta de solo no campo. Sociedade Brasileira de Ciência do Solo – Centro Nacional de Pesquisa de Solos. 3ª ed., Campinas-SP. 83.

Liang S (2021) Narrowband to broadband conversions of land surface albedo I: Algorithms. Remote Sens. Environ., Amsterdan, 76 (2) 213-238.

Malavolta E, Vitti GC, Oliveira AS (1997) Avaliação do estado nutricional das plantas: princípios e aplicações. 2. Ed. Piracicaba: POTAFOS, 319.

Medrado E, Lima JEFW (2014) Development of pedotransfer functions for estimating water retention curve for tropical soils of the Brazilian savanna. Geoderma Regional, Amsterdam, 1 (1) 59-66.

Mussi RF, Alves Jr J, Evangelista AWP, Casaroli D, Battisti R (2020) Evapotranspiração da cana-de-açúcar estimada pelo algoritmo SAFER. Irriga, Botucatu, 25 (2) 263-278.

Nádudvari A, Abramowicz A, Fabianska M, Misz-Kennan M, Ciesielczuk J (2020) Classification of fires in coal waste dumps based on Landsat, Aster thermal bands and thermal camera in Polish and Ukrainian mining regions. Inter. J. Coal Sci. & Tech. 8 (3) 441-456.

Oliveira DA, Hernandez FBT, Bispo RC, Gomes RN, Teixeira AHC (2021) Estimativa da demanda de água da cultura da cana-de-açúcar irrigada utilizando sensoriamento remoto. Irriga, Botucatu, 1 (4) 678-686.

Ometto JC (1981) Bioclimatologia Vegetal. São Paulo: Ed. Agronômica Ceres, 440.

Queiroz HAA, Brito CVO (2022) Assessment of Landsat and Sentinel images integration for surface water extent mapping. Rev. Bras. Geom., Curitiba 10 (1) 3-19.

Sales DLA, Alves Jr J, Souza JMF, Casaroli D, Evangelista AWP, Pereira RM (2016) Common bean evapotranspiration estimated by orbital images. Afr. J. Agric. Res., Cape Coast, 11 (1) 867-872.

Sales DLA, Alves Jr J, Casaroli D, Evangelista AWP, Souza JMF (2017) Estimativa de evapotranspiração e coeficiente de cultura do tomateiro industrial utilizando o algoritmo SAFER. Irriga, Botucatu, 22 (3) 629-640.

Sena CC, Alves Jr J, Domingos MVH, Antunes Jr EJ, Battisti R, Evangelista A WP, Casaroli D (2020) Calibração do sensor capacitivo de umidade do solo EC-5 em resposta a granulometria do solo. Braz. J. Dev., Curitiba, 6 (4) 17228-17240.

Souza JMF, Alves Jr J, Casaroli D, Evangelista AWP, Mesquita M (2020) Validação do modelo SAFER na estimativa da evapotranspiração da cana-de-açúcar. Irriga, Botucatu, 25 (2) 247-262.

Stone LF, Silveira PM, Moreira JAA, Braz AJBP (2006) Evapotranspiração do feijoeiro irrigado em plantio direto sobre diferentes palhadas de culturas de cobertura. Pesqui. Agropecu. Bras., Brasília, 41 (4) 577-582.

Teixeira AHC (2010) Determining Regional Actual Evapotranspiration of Irrigated Crops and Natural Vegetation in the São Francisco River Basin (Brazil) Using Remote Sensing and Penman-Monteith Equation. Remote Sens., Basel, 2 (4) 1287-1319.

Teixeira AHC, Hernandez FBT, Lopes HL (2012) Application of Landsat images for quantifying the energy balance under conditions of fast land use changes in the semi-arid region of Brazil. In: SPIE Remote Sensing, 2012, Edinburgh. Proc. SPIE 8531, Remote Sensing for Agriculture, Ecosystems, and Hydrology, XIV, (8531) 1-10. Disponível em: <ftp://ftp.feis.unesp.br/agr/pdf/heriberto_safer_landsat.pdf> Acesso em: 04 de julho 2020.

Teixeira A, Pacheco E, Silva CS, Dompieri M, Leivas J (2021) SAFER applications for water productivity assessments with aerial camera onboard a remotely piloted (RPA). A rainfed corn study in Northeast Brazil. Remote Sensing Applications: Soc. Environ., Amsterdan, 22 (1) 1-15.

Thornthwaite CW, Mather JR (1955) The water balance. Publications in Climatology, New Jersey, Drexel Inst. of Technology. 104.

Planck M (1901) Ueber das Gesetz der Energieverteilung im Normalspectrum. Annalen der Physik. 19 (1), 202-237.

Willmott CJ, Ackleson SG, Davis RE, Feddema JJ, Klink KM, Legates DR, O'Donnell J, Rowe CM (1985) Statistics for the evaluation and comparison of models. J. Geophys. Res., Ottawa, 90 (1) 8995-9005.